Cell, Vol. 109, 437–446, May 17, 2002, Copyright ©2002 by Cell Press

Microarray Deacetylation Maps Determine Genome-Wide Functions for Yeast Histone Deacetylases

Daniel Robyr,[1] Yuko Suka,[1] Ioannis Xenarios,[2] Siavash K. Kurdistani,[1] Amy Wang,[1] Noriyuki Suka,[1] and Michael Grunstein[1,3]

[1]Department of Biological Chemistry
UCLA School of Medicine and the Molecular Biology Institute
Boyer Hall
[2]UCLA-DOE Laboratory of Structural Biology and Molecular Medicine
University of California, Los Angeles
Los Angeles, California 90095

Summary

Yeast contains a family of five related histone deacetylases (HDACs) whose functions are known at few genes. Therefore, we used chromatin immunoprecipitation and intergenic microarrays to generate genome-wide HDAC enzyme activity maps. Rpd3 and Hda1 deacetylate mainly distinct promoters and gene classes where they are recruited largely by novel mechanisms. Hda1 also deacetylates subtelomeric domains containing normally repressed genes that are used instead for gluconeogenesis, growth on carbon sources other than glucose, and adverse growth conditions. These domains have certain features of heterochromatin but are distinct from subtelomeric heterochromatin repressed by the deacetylase Sir2. Finally, Hos1/Hos3 and Hos2 preferentially affect ribosomal DNA and ribosomal protein genes, respectively. Thus, acetylation microarrays uncover the "division of labor" for yeast histone deacetylases.

Introduction

Nucleosomal repression of eukaryotic promoters is regulated by histone acetylation and deacetylation. The complexity of this regulation is illustrated by the presence of at least five related histone deaceylases (HDACs) in the simple eukaryote *Saccharomyces cerevisiae*. This yeast contains not only HDACs Rpd3, Hda1, Hos1, Hos2, and Hos3 that are related by sequence, but also the relatively unrelated heterochromatin bound deacetylase Sir2 and enzymes Hst1-4 that have similarity to Sir2 (Moazed, 2001; Rundlett et al., 1996). Where and how the HDACs deacetylate chromatin genome-wide is unknown. Previous functional analyses have focused on few HDACs and even then only on a gene-by-gene basis. For example, Rpd3, the prototype for the mammalian class I histone deacetylases (e.g., HDAC 1-3) is recruited by DNA binding Ume6 protein to the URS1 elements of the yeast *INO1* and *IME2* genes (Kadosh and Struhl, 1997). Chromatin immunoprecipitation (ChrIP or ChIP) with antibodies to acetylated lysine residues has shown that Rpd3 strongly deacetylates all four core histones at approximately two nucleosomes adjacent to these URS1 elements (Kadosh and Struhl, 1998; Rundlett et al., 1998; Suka et al., 2001). Similarly, Hda1, the prototype for the mammalian class II histone deacetylases (HDAC 4-6), is recruited by yeast Tup1 protein. Tup1 is in turn targeted to URS elements of loci such as the stress response *ENA1* gene by specialized DNA binding proteins (e.g., Mig1 and Sko1). At *ENA1*, Hda1 deacetylates histone H3 and H2B sites only at 2–3 nucleosomes adjacent to the URS to help repress gene activity (Wu et al., 2001). Thus, two quite distinct HDACs, Rpd3 and Hda1, are similarly recruited (by different factors) to URS elements to deacetylate adjacent nucleosomes (albeit different histone classes). However, this simple view of HDAC function is derived from few HDAC sites of activity. In fact, Rpd3/Hda1 disruptions also lead to increased acetylation throughout the acid phosphatase *PHO5* gene even though there are no known binding sites for Ume6 or Tup1 at *PHO5* (Vogelauer et al., 2000). This latter form of deacetylation affects promoter and coding regions at multiple genomic sites lacking URS elements and has been termed "global deacetylation" (Vogelauer et al., 2000; Wu et al., 2001). Therefore, we believe that a genome-wide analysis is necessary if we are to have a comprehensive understanding of the functions of Rpd3 and Hda1 as well as Hos1, Hos2, and Hos3, whose functions are virtually unknown. Only in this way can we begin to understand the variety of gene targets, recruitment mechanisms, and enzymatic activities that are involved in the diverse functions of the yeast family of deacetylases.

Genome-wide analyses should ideally involve three tools: (1) enzyme binding arrays, to determine where in the genome HDACs recognize chromatin; (2) acetylation arrays to determine where histones are acetylated; and (3) expression arrays, to determine where gene activity is altered by the disruption of HDACs. In this manner, one could more easily distinguish between direct and indirect effects of histone deacetylases on gene expression. Such arrays should also distinguish between sites of HDAC binding and sites of activity which a priori need not be identical. Expression microarrays resulting from disruption of HDACs have been described (Bernstein et al., 2000; Hughes et al., 2000). Also, we have recently generated enzyme binding microarrays demonstrating the interaction of Rpd3 deacetylase genome-wide (Kurdistani et al., 2002). In the paper below, we describe acetylation microarrays. These genome-wide maps of enzyme activities have allowed us to identify different gene and histone targets for the entire yeast HDAC family.

Results

Acetylation Microarrays

Chromatin immunoprecipitation (ChrIP or ChIP) has recently been coupled with DNA microarrays in order to determine protein binding sites genome-wide (Iyer et al., 2001; Ren et al., 2000). We have adapted this ap-

[3]Correspondence: mg@mbi.ucla.edu

proach to the study of genome-wide histone deacetylation (see Supplemental Figure S1 at http://www.cell.com/cgi/content/full/109/4/437/DC1). Chromatin fragments from formaldehyde-treated histone deacetylase mutant cells and their wild-type isogenic counterparts were immunoprecipitated using highly specific antibodies against selected acetylated histone sites that we believe to be representative (Suka et al., 2001; White et al., 1999; Wu et al., 2001). DNA from enriched chromatin fragments was purified, amplified by PCR, and labeled with a fluorophore (Cy3 or Cy5). Wild-type (wt) and mutant sets of labeled DNA were then combined and hybridized to a DNA microarray containing ~6700 intergenic regions (IGRs) that were amplified in our laboratory using primer sets from Research Genetics (Invitrogen) (Iyer et al., 2001). IGRs were chosen for this study since they contain the URS elements that recruit deacetylases (Kadosh and Struhl, 1997; Wu et al., 2001). For a given IGR, the ratio of the normalized fluorescent intensities between the two probes indicates whether the analyzed lysine residue is hypo- or hyperacetylated upon deletion of a deacetylase gene (as compared to the wt strain). IGRs located between two convergent genes do not contain promoter sequences and as a consequence are not assigned to a particular open reading frame (ORF). On the other hand, IGRs shared by two divergent genes cannot be assigned unambiguously to one particular ORF. Therefore, we considered by default that a change of acetylation at these regions potentially affects both ORFs. Moreover, large IGRs were split into smaller regions of about 1 kb on the DNA microarray, leading to the creation of intergenic fragments surrounded by two or more other intergenic regions. These internal regions that are not assigned to an ORF are referred to as orphans. Using acetylation microarrays, we investigated the IGRs affected by deacetylase mutations in yeast.

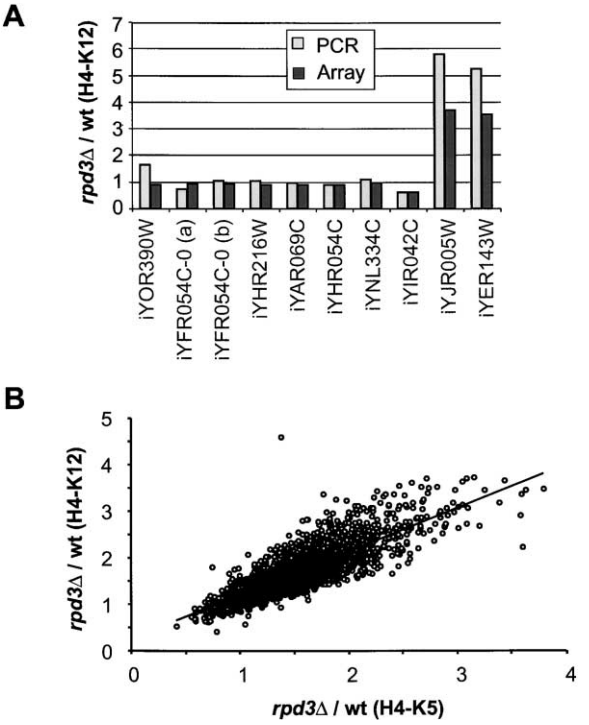

Figure 1. Acetylation Microarrays and Standard ChrIP Show Similar Patterns of Acetylation

(A) Intergenic regions acetylated at H4 K12 were selected randomly from our *rpd3*Δ microarray data and checked by standard ChrIP using multiplex PCR. The normalized immunoprecipitation ratios of acetylated K12 between *rpd3*Δ and wild-type strains are plotted for each selected region (array data, dark bars; PCR from ChrIP, light bars). The large intergenic region iYFR054C-0 (1132 bp on chromosome 6 between coordinates 259421 and 260552) in the array was analyzed by PCR at two different locations (a, 259431 to 259686; b, 260067 to 260290).

(B) Graph plotting increased acetylation caused by *rpd3*Δ at H4-K5 versus H4-K12. The numbers on both axes correspond to the ratios of the normalized fluorescence intensities between *rpd3*Δ and wild-type (wt).

RPD3 Genome-Wide Histone Deacetylation

Rpd3 has been shown to deacetylate histone H4 lysines K5, K8, and K12 (more so than K16) at the *INO1* and *IME2* promoters (Kadosh and Struhl, 1998; Rundlett et al., 1998; Suka et al., 2001). Therefore, to investigate genome-wide deacetylation by Rpd3, we used an antibody against histone H4 K12 (Suka et al., 2001) in acetylation microarrays to determine where in the genome H4 K12 is hyperacetylated upon disruption of *RPD3* (*rpd3*Δ). To confirm that the data of the acetylation microarrays is reliable, ten different IGRs acetylated upon deletion of *RPD3* were picked randomly and checked by standard ChrIP. We found for all ten regions that relative acetylation at H4 K12 upon *rpd3*Δ is similar in the microarray and in standard ChrIP (Figure 1A). As mentioned above, *rpd3*Δ increases H4 K12 and K5 acetylation in a similar manner at the *INO1* and *IME2* promoters (Suka et al., 2001). Therefore, acetylation at these two lysines for all yeast genes in the arrays were compared (Figure 1B). We observe that the two sets of data correlate well (correlation coefficient 0.83). Thus, we conclude from these two approaches that acetylation microarrays can be used with confidence to assay for increased acetylation, and therefore deacetylase activity, genome-wide.

We arbitrarily set the relevant H4 K12 (or K5) acetylation increase resulting from *RPD3* disruption at a cutoff of 1.95-fold for the purpose of data analysis. This cutoff is conservative, as shown by the low level of variation in H4 K12 acetylation in the wt strain.

The average enrichment of acetylated H4 K12, when compared for Cy3- versus Cy5-labeled wt DNAs on the same slide, is 1.06 (standard deviation 0.09) with all values for IGRs ranging from 0.68-fold to 1.45-fold (data not shown). In contrast, we find 815 IGRs whose H4 K12 acetylation is increased 1.95-fold or more when *RPD3* is deleted (see Supplemental Figure S2 at http://www.cell.com/cgi/content/full/109/4/437/DC1). Included amongst these sites are promoters for 531 different ORFs. While *RPD3* affects the acetylation of genes in virtually all cellular pathways (see Supplemental Table S1), there is a modest overrepresentation of genes that take part in sporulation, germination, and meiosis ($p = 1.3 \times 10^{-3}$). There is also a significant preference for genes throughout the genome that are involved in carbohydrate utilization. These include genes involved in car-

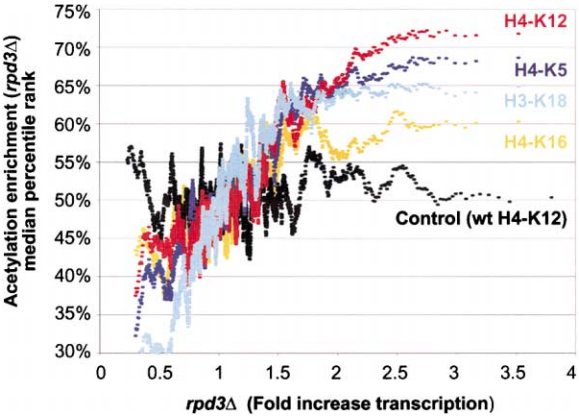

Figure 2. Histone H4 K5 and K12 Acetylation Correlate Best with Increased Transcription Resulting from *rpd3*Δ

The moving average (window size, 100 IGRs; step, 1 IGR) percentile rank of acetylation enrichment is plotted as a function of transcription increase resulting from *rpd3*Δ (Bernstein et al., 2000). Acetylation data are plotted for H4 K5 (dark blue), H4 K12 (red), H4 K16 (orange), and H3 K18 (light blue). Control corresponds to a comparison of two sets of probes amplified from the immunoprecipitation of acetylated H4 K12 in the wt strain and labeled separately with Cy-3 and Cy-5 prior to hybridization.

bohydrate transport ($p = 8.5 \times 10^{-7}$) and metabolism ($p = 1.5 \times 10^{-3}$) as well as energy reserves ($p = 6.7 \times 10^{-3}$).

Rpd3 has been described to be a repressor (Kadosh and Struhl, 1997), and yet *RPD3* deletion results in more genes being downregulated than upregulated in expression microarrays, leading to speculation as to its possible role as an activator (Bernstein et al., 2000). To investigate this possibility, we compared the effects of *rpd3*Δ on acetylation and expression microarrays. Of the original pool of 531 promoters for ORFs affected by *rpd3*Δ in the acetylation microarrays, data for 493 ORFs are available in the expression array (Bernstein et al., 2000). As many as 65 of these 493 ORFs (13%) that may be deacetylated by Rpd3 are significantly upregulated (>2-fold) by *rpd3*Δ ($p = 1.2 \times 10^{-19}$). However, there is little significant overlap between genes whose acetylation is increased by *rpd3*Δ and those that are downregulated >2-fold. Only 24 of the 493 ORFs (4.9%) are hyperacetylated and further repressed by *rpd3*Δ ($p = 0.215$). We conclude that our data support a role for Rpd3 as a repressor only and that most genes that are downregulated in the *rpd3*Δ strain are likely to be affected indirectly by the mutation.

We then asked whether there is a correlation between the hyperacetylation of specific H4 or H3 lysines and increased transcription resulting from *rpd3*Δ. Comparing our data to that of *rpd3*Δ expression microarrays (Bernstein et al., 2000), we find that increased acetylation at histone H4 K5 and K12 is associated most directly with increased gene activity (Figure 2). Interestingly, H3 K18 acetylation and transcription associate less well genome-wide despite very strong effects of *rpd3*Δ on H3 acetylation at the *INO1* promoter (Suka et al., 2001). Finally, increased acetylation of H4 K16 and increased gene activity show the poorest correlation. These data indicate that different histone acetylation sites can have different roles in genome-wide gene regulation.

Since Ume6 recruits Rpd3 to the *INO1* promoter, we wished to know whether most promoters affected by *RPD3* contain Ume6 binding sites. For this comparison we separated the 531 affected IGRs in different categories as a function of acetylation fold increase and analyzed their sequences for the presence of a consensus Ume6 binding URS1 NTNGCCGCC site using the web RSA Tools package (van Helden et al., 2000) (http://www.ucmb.ulb.ac.be/bioinformatics/rsa-tools/). We find that 13% and 21% of IGRs whose H4 K12 acetylation is increased by 1.95- to 2.5-fold and 2.5- to 3.0-fold by *rpd3*Δ, respectively, contain a possible Ume6 binding site. This is increased to 43% when analyzing IGRs whose acetylation is increased >3-fold by *rpd3*Δ (Table 1). Therefore, IGRs whose acetylation is increased most strongly by *rpd3*Δ are the most likely to contain Ume6 binding sites. Yet, even of this group, 57% do not contain recognition sites for Ume6. These data indicate that Ume6 has a special role in deacetylation by Rpd3; however, most promoters affected by Rpd3 must use other mechanisms to recruit the deacetylase. Similar conclusions were obtained by examining the binding of Rpd3 and Ume6 genome-wide (Kurdistani et al., 2002).

HDA1 Genome-Wide Deacetylation

Hda1 specifically deacetylates all acetylation sites examined in histones H3 and H2B only (Wu et al., 2001). Therefore, to determine the genome-wide roles of Hda1, we examined the effect of *hda1*Δ on the acetylation of H3 K9 and K18 and H2B K16 acetylatable lysines. We find that 647 IGRs are hyperacetylated at H3 K18 when *HDA1* is deleted. Their genes, illustrated in this case across a chromosomal map of the yeast genome (Figure 3, red boxes), affect most cellular functions throughout the genome (see Supplemental Table S1 at http://www.cell.com/cgi/content/full/109/4/437/DC1). However, Hda1 does have preference for genes involved in drug transport ($p = 4.3 \times 10^{-4}$), detoxification ($p = 7.9 \times 10^{-4}$), stress response ($p = 1.3 \times 10^{-3}$), and cell wall function ($p = 1.9 \times 10^{-6}$). Hda1 also preferentially targets the class of genes that regulates carbohydrate utilization such as those involved in carbohydrate transport ($p = 8.0 \times 10^{-5}$) and metabolism ($p = 3.0 \times 10^{-6}$) as well as energy reserves ($p = 1.5 \times 10^{-4}$). Some of these are affected by Rpd3 ($p = 2.7 \times 10^{-4}$ for the carbohydrate utilization genes). Genome-wide, 139 IGRs are affected by both Hda1 and Rpd3. This represents ~23% of the Hda1-affected regions and ~19% of Rpd3-affected sites ($p = 3.4 \times 10^{-7}$). Therefore, the acetylation of the majority of these promoters (~73% of Hda1-affected sites, ~81% of Rpd3-affected sites) is affected mainly by either Hda1 or Rpd3.

In the case of acetylation sites affected by *hda1*Δ, acetylation of H3 K9, H3 K18, and H2B K16 correlate in a very similar manner with increased transcription resulting from *hda1*Δ (Figure 4A). Curiously, there are certain promoters (e.g., for *YOR223W*, *YDR057W*, *ADH1, MRS6, MRC1*, *PAF1*, and *SIR3*) whose histone H2B is hyperacetylated ~2- to 3-fold in the *hda1*Δ strain that are paradoxically downregulated in the *hda1*Δ mutant (Figure 4A, arrow). It is formally possible that Hda1 is a direct activator of these promoters. However, to do so Hda1 must deacetylate H2B (and not H3) at these genes

Table 1. Many Promoters Affected by *RPD3* Deletion Do Not Contain Ume6 Consensus DNA Binding Sites

Increase of acetylation at H4-K12	Number of Affected Promoters	Number of Affected Promoters with Potential Ume6 Binding Sites	Fraction of Affected Promoters with Ume6 Sites
From 1.95- to 2.5-fold	407	54	13.3%
From 2.5- to 3.0-fold	87	18	20.7%
Above 3-fold	37	16	43.2%
Total	531	88	16.6%

Number of promoter regions affected on histone H4 K12 by *RPD3* depletion and which contain at least one potential Ume6 DNA binding site (NTNGCCGCC). A computer search for the consensus Ume6 DNA binding site NTNGCCGCC upstream of all yeast ORF (−10 to −800) was performed using the web RSA Tools package (http://www.ucmb.ulb.ac.be/bioinformatics/rsa-tools/). The number of "NTNGCCGCC"-containing promoter regions that are deacetylated by Rpd3 was then calculated for each category (fold increase). The fraction of Ume6-containing regions deacetylated by Rpd3 is underestimated since we have arbitrarily assigned a Ume6 site to only one ORF for genes that share the same intergenic region.

despite its specificity for both H3 and H2B at other sites examined (this paper, and Wu et al., 2001). Alternatively, it is possible that *HDA1* deletion directly or indirectly affects a secondary modification of H2B at these genes only, resulting in their downregulation. Since H2B is specifically ubiquitinated in yeast (Robzyk et al., 2000), it is conceivable that Hda1 regulates H2B ubiquitination (or another H2B-specific function) that preferentially affects the expression of a limited number of genes.

We have shown that Hda1 is recruited through the repressor Tup1 to deacetylate the promoter of the *ENA1* gene while Rpd3 deacetylates its coding region in a global manner (Wu et al., 2001). However, other studies (Watson et al., 2000) have proposed that only when three class I deacetylases (Rpd3, Hos1, and Hos2) are disrupted is there an effect on acetylation of the *STE6* gene in *MAT*α cell in which *STE6* is repressed. These latter findings would argue that Hda1 is not involved in

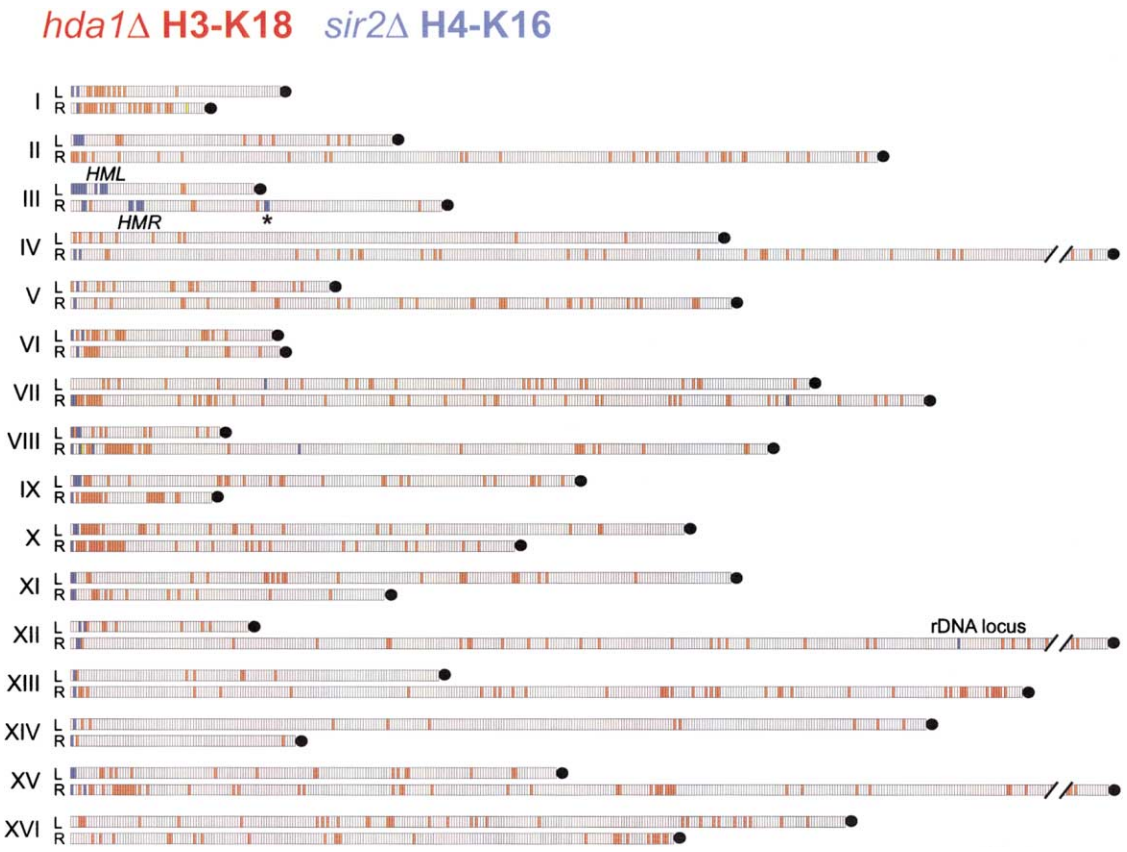

Figure 3. Chromosomal Display of Sites Affected by *HDA1* at Histone H3 K18 and Sir2 at H4 K16

Left (L) and right (R) chromosome arms are represented from their telomere end to their centromere (black circle). Each intergenic region is illustrated by a rectangle. Regions whose enrichment is increased relative to the control are shaded either in red (>1.95) for Hda1 or blue (>1.5) for Sir2. Sites affected by both Hda1 and Sir2 are yellow. The location of the mating type *HMR* and *HML* loci as well as of the rDNA locus are indicated. Possible deacetylation by Sir2 at the *MAT* locus on chromosome 3 (depicted by a star) is probably an artifact due to crosshybridization with the silent copy at *HMR* that is affected by Sir2. Note that chromosomes are not to scale since ORFs were left out and intergenic regions were arbitrarily given the same width for clarity. Large chromosomes were trimmed.

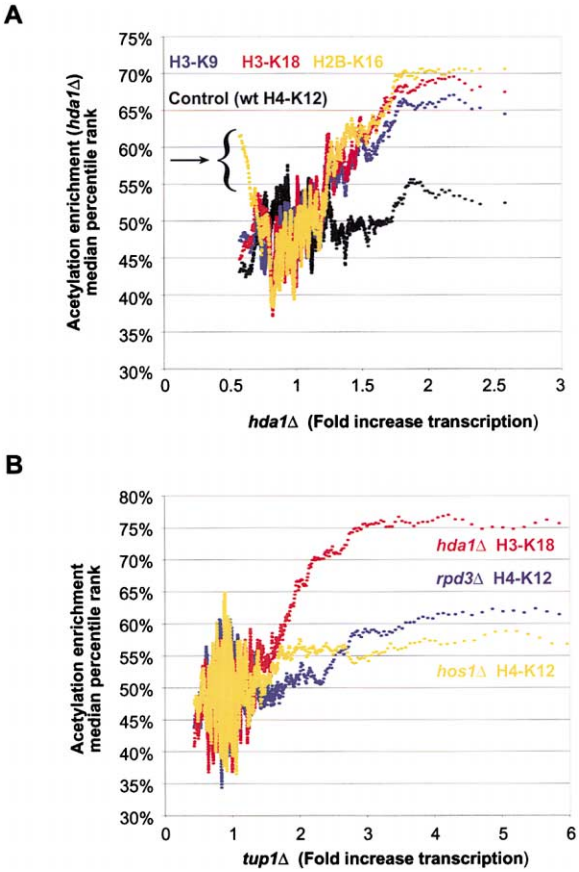

Figure 4. Genome-Wide Relationship between Increased Transcription and Acetylation Site Usage

(A) Relationship between increased transcription and acetylation site usage upon deletion of *HDA1*. The moving average (window size, 100; step, 1) percentile rank of acetylation enrichment is plotted as a function of transcription increase resulting from *hda1*Δ (Bernstein et al., 2000). Acetylation data are plotted for H3 K9 (dark blue), H3 K18 (red), and H2B K16 (orange). Control is as in Figure 2.

(B) Tup1-regulated promoters are uniquely deacetylated by Hda1. The moving average (window size, 100; step, 1) percentile rank of acetylation enrichment (*hda1*Δ) is plotted as a function of expression changes in *tup1*Δ (DeRisi et al., 1997). Acetylation data are plotted for *rpd3*Δ H4 K12 (dark blue), *hda1*Δ H3 K18 (red), and *hos1*Δ H4-K12 (orange).

regulation by Tup1. To determine whether repression by Tup1 is associated genome-wide preferentially with Hda1, Rpd3, or Hos1 deacetylation, we compared (Figure 4B) the data of the acetylation microarrays with *tup1*Δ expression microarrays (DeRisi et al., 1997). We find that hyperacetylation caused by *hda1*Δ correlates very well with increased expression resulting from *tup1*Δ. In contrast, there is poor correlation of hyperacetylation caused by *rpd3*Δ or *hos1*Δ with expression resulting from *tup1*Δ. We also have found that *TUP1* deletion (and *HDA1* deletion) causes an increase in the acetylation of histone H3 sites but not those of H4 at the *STE6* promoter in *MAT*α cell (J. Wu and M.G., unpublished). Thus, even at *STE6*, Tup1 is unlikely to recruit Rpd3 (that is required for deacetylating both H3 and H4) to the promoter. Therefore, it is possible that class I deacetylases have global rather than promoter-specific roles at genes such as *STE6*. In conclusion, our data indicate that Tup1 recruits Hda1 deacetylase preferentially to IGRs genome-wide.

While Tup1 recruits Hda1 preferentially (acetylation of ~43% of the Tup1-regulated promoters genome-wide [Hughes et al., 2000] is increased by *hda1*Δ [$p = 2.3 \times 10^{-63}$]), it is possible that most Hda1 is not recruited by Tup1. In fact, we find that ~69% of the IGRs affected by Hda1 are not upregulated by *TUP1* deletion. It is reasonable to assume, based on expression arrays of *tup1*Δ strains (DeRisi et al., 1997) and analysis of individual Tup1-regulated genes (Wu et al., 2001; Davie et al., 2002), that Tup1 is involved in both the recruitment of Hda1 and subsequent repression at these genes. Given this assumption, our data argue that Hda1 recruitment to most IGRs occurs through factors other than Tup1.

Histone Deacetylation of Distinct Chromosomal (HAST) Domains

We then asked whether Hda1 and Rpd3 may function not only at individual IGRs genome-wide but in some cases at distinct chromosomal domains. To address this question, IGRs were sorted by their distance from the telomere in groups of 100. In each group, the fraction of hyperacetylated sites upon deletion of *HDA1* or *RPD3* was plotted as a function of distance from the telomere (Figure 5A). We find that *hda1*Δ affects acetylation preferentially at ~10–25 kilobases (kb) from the telomeres, while *rpd3*Δ affects IGRs genome-wide in a much more uniform manner with a lesser effect in the subtelomeric region. These data indicate that gene clusters that are deacetylated by Hda1 may exist at ~10–25 kb from the telomere. We have identified 22 chromosome ends with such domains having sizes that range from ~4 kb at Chr. XI-R to ~34 kb at Chr. X-R (see Supplemental Table S2 at http://www.cell.com/cgi/content/full/109/4/437/DC1). Interestingly, many subtelomeric regions affected by Hda1 appear to be contiguous. Not only are IGRs affected, but the adjacent orphans in these regions are affected as well. Moreover, when we examined the hyperacetylation of ORF microarrays (obtained from Corning) using similar approaches, we found that many of the ORFs between the IGRs are hyperacetylated by deletion of *HDA1*. This is shown for Chr. IX-R (inset) in Figure 5A in which stars designate ORFs. Therefore, the subtelomeric regions, whose acetylation is affected by Hda1, include adjacent IGRs, orphans, and ORFs, and are likely to contain continuous stretches of Hda1-deacetylated chromatin. We refer to the Hda1-affected subtelomeric regions as HAST domains.

To identify the role of HAST domains in cellular physiology, we first examined the regulation of specific genes and gene classes in these chromosomal regions. By comparing steady-state RNA expression levels (Holstege et al., 1998) to the acetylation microarrays, we found that the 149 genes in HAST domains have transcript levels that are on average less than 1 molecule per cell (0.8 molecules mRNA/HAST gene/cell in YPD or glucose medium). The HAST genes are significantly ($p = 4.1 \times 10^{-24}$) less active than the genome as a whole whose average transcript level (including repressed and activated genes) is ~2.7 molecules of mRNA/gene/cell. Since yeast cells normally utilize glucose and oxygen,

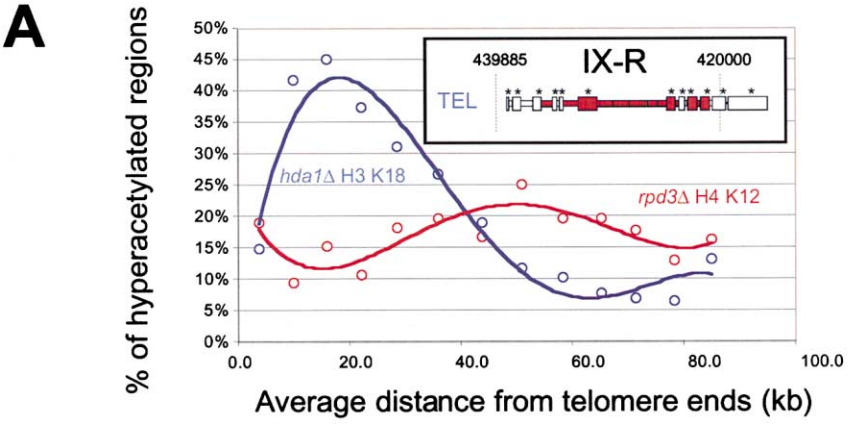

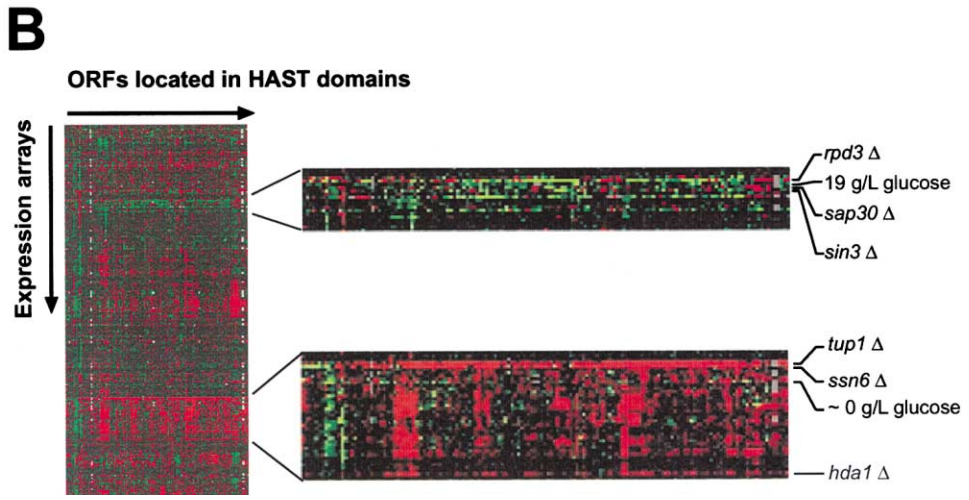

Figure 5. Identification of Subtelomeric HAST Domains that Are Regulated by Hda1 and Tup1/Ssn6

(A) Hda1 affects the acetylation of H3 K18 at subtelomeric domains preferentially. All intergenic fragments were sorted in groups of 100 as a function of their distance from the telomere. Shown are the percent of fragments within each group that are hyperacetylated at H3 K18 by *hda1*Δ (blue line) and *rpd3*Δ at H4-K12 (red line) plotted against their average distance (kb) from a telomere. The inset is a chromosomal display of a subtelomeric domain affected by *HDA1* (red rectangles) on chromosome IX-R. ORFs are designated by stars. The telomere (TEL) and the chromosome coordinates are also indicated.

(B) Hda1-affected subtelomeric domains are repressed by Tup1, Ssn6, and Hda1. Hierarchical cluster analysis comparing expression data from 300 mutants or conditions (Hughes et al., 2000) with 149 ORFs located in the HAST domains. Only a portion of the analysis is shown for clarity. The scale of gene activity is represented from green (repressed) to red (derepressed). The cluster analysis was performed with Gene cluster (2.11) and visualized using TreeView (1.50) (Eisen et al., 1998).

we pursued the possibility that HAST domain genes may function primarily in alternate conditions of environmental stress. This hypothesis is strongly supported by the finding that *PCK1* (phosphoenolpyruvate carboxykinase), the key regulator of gluconeogenesis, which is activated upon glucose depletion, is found in a HAST domain on Chr. XI-R.

The various HAST domains also contain genes such as *MAL11*, *MAL12*, *MAL13*, *MAL31*, *MAL32*, *MAL33*, *PEX11*, *HXK1*, and *PGU1* for maltose and alternate carbon source utilization and fermentation; *GRE2*, *AQY1*, *AQY2*, *YPS6*, *FET4*, *FIT2*, *FIT3*, *DAN1*, *DAN4*, *PHO89*, *ARN1*, *ENB1*, *GTT1*, and *GDH3* for growth under adverse environmental conditions such as osmotic shock, starvation, and sexual reproduction, anaerobic growth, changes in pH, drug resistance, iron starvation, haploid invasive growth, and stress response. HAST domains also include *BIO3*, *BIO4*, and *BIO5* that are involved in biotin biosynthesis, a prosthetic group required for pyruvate carboxylase function in gluconeogenesis. Interestingly, the genes for many hexose transporters (including *HXT8*, *HXT11*, and *HXT12*) are present in the HAST domains. However, these are minor transporters in high glucose, conditions under which non-HAST Hxt1 and Hxt3 are used primarily (Boles and Hollenberg, 1997). The main function of the minor transporters may be to transport other sugars (e.g., mannose) (Boles and Hollenberg, 1997), which would explain their repression or downregulation in high glucose. Decreased Hda1 levels are expected to help activate HAST genes (below). Interestingly, *HDA1* itself is downregulated during the diauxic shift (DeRisi et al., 1997), as the cell adapts its transcriptional program in order to survive nutrient depletion, in particular glucose. Taken together, the

above data argue that a major function of HAST domains is to repress genes that are subsequently activated by alternate carbon sources and adverse conditions of growth.

In order to determine under which conditions the HAST domain genes may be coregulated, we examined expression of the 149 HAST ORFs under ~300 different conditions (Hughes et al., 2000). As shown in Figure 5B, *TUP1*, *SSN6*, and *HDA1* deletion preferentially cause increased expression of ORFs in the HAST domains (see Supplemental Figure S3 at http://www.cell.com/cgi/content/full/109/4/437/DC1 for full analysis). Hda1 has a clear but lesser effect on transcription in line with earlier data showing that *HDA1* deletion alone does not fully derepress *ENA1* (Wu et al., 2001). Tup1 and Ssn6 strongly affect repression of most HAST genes since they are derepressed on average 7.6-fold by *TUP1* deletion and 33.8-fold by *SSN6* deletion (Hughes et al., 2000). These effects are 5- to 6-fold greater than the effects of these deletions on genes of the genome as a whole (1.5- and 5.8-fold derepression, respectively). Therefore, Tup1/Ssn6 are likely to be involved in recruiting Hda1 to HAST domain genes. Interestingly, although Tup1/Ssn6 are most likely the common repressors for the HAST domain genes, there may not be a single induction mechanism. On the contrary, specific groups of HAST genes can be activated independently from one another in different conditions, such as growth in low glucose (Figure 5B; see Supplemental Figure S3).

Heterochromatin and HAST Domains

Heterochromatin-like regions formed through the interactions of Sir3 and Sir4 proteins as well as the NAD-dependent histone deacetylase Sir2 are also present at subtelomeric regions. We wished to know whether such regions overlap with HAST domains. *SIR* gene disruption results in heterochromatin hyperacetylation (Braunstein et al., 1996; Suka et al., 2001), and Sir2 deacetylates H4 K16 in vitro (Imai et al., 2000). Therefore, we used acetylation microarrays to determine where H4 K16 is acetylated genome-wide upon disruption of *SIR2*. As shown in Figure 3, *sir2*Δ leads to hyperacetylation of subtelomeric sequences (blue boxes) very close to the telomeric ends (generally less than 4 kb) as well as other regions known to bind Sir2 (the silent mating loci *HML*, *HMR*, and the rDNA locus) (Moazed, 2001; Strahl-Bolsinger et al., 1997). However, we find that there is virtually no overlap between these Sir2-affected regions and the HAST domains (Figure 3).

Unexpectedly, deletion of the repressor *RPD3* (or associated factors *SIN3* and *SAP30*) improves silencing at HAST domain genes (see Supplemental Figure S3 at http://www.cell.com/cgi/content/full/109/4/437/DC1). This effect is reminiscent of that showing that *rpd3*Δ also improves silencing of telomeric and *HM* heterochromatin that utilizes Sir proteins (De Rubertis et al., 1996; Rundlett et al., 1996; Vannier et al., 1996). However, this effect of *rpd3*Δ on HAST genes and on yeast heterochromatin may be indirect, as we do not find a significant overlap ($p = 0.459$) between decreased transcription at these sites (Bernstein et al., 2000) and increased acetylation caused by *rpd3*Δ (see Supplemental Figure S3).

Hos1, Hos2, and Hos3 Deacetylases Affect Ribosomal DNA and Ribosomal Protein Genes

The functions of the *HOS* deacetylases and their gene targets have been unclear. However, we have found using acetylation microarrays that *HOS1* and *HOS3* are required for the deacetylation of histone H4 K12 preferentially at a very limited number of intergenic sites mainly on Chr. XII-R (Figure 6). Of the 15 regions affected 1.95-fold or more by *hos1*Δ, 11 are in the rDNA locus (Figure 6). Similar results were obtained for *hos3*Δ at both H4 K12 and H2B K16. Since it may be argued that *hos1*Δ and *hos3*Δ result in increased rDNA copy number, we examined this possibility in the mutants. Using PCR we find no discernable effect of either *hos1*Δ or *hos3*Δ on rDNA copy number (data not shown). Interestingly, despite having global functions, *RPD3* and *HDA1* disruptions do not alter acetylation of the rDNA sites in an obvious manner. It should be noted that *HDA1* disruption leads to a reduction of the rDNA copy number (~2-fold) as tested by comparing input genomic DNA from the disrupted and wt strains using microarrays (data not shown). Thus, the apparent ~2-fold reduction in acetylation at the rDNA locus in the *hda1*Δ strain (see Supplemental Data at http://www.uclaaccess.ucla.edu/labs/grunstein/acetyl.html) is likely due to the reduction in rDNA copy number. Since the transcription of approximately 50% of rDNA repeats is repressed by unknown mechanisms (Lucchini and Sogo, 1994), these data suggest the possibility that Hos1 and Hos3 are involved in rDNA repression.

Acetylation microarrays demonstrate that *HOS2* is also required for deacetylation of histone H4 K12. The acetylation increase is at most ~1.7-fold in the *hos2*Δ strain in these experiments. However, there is an overrepresentation of 22 ribosomal protein (RP) genes among the 75 fragments whose acetylation is affected the most by *hos2*Δ ($p = 1.9 \times 10^{-16}$) (see Supplemental Table S3 at http://www.cell.com/cgi/content/full/109/4/437/DC1). Interestingly, among the top ten loci at the top of our list, four are ribosomal protein ORFs (*RPL28*, *RPS19B*, *RPL27A*, and *RPS27B*) (our acetylation arrays contain several ORFs in addition to intergenic regions). Therefore, *HOS2* is required for the preferential deacetylation of RP genes under these conditions. In summary, the three *HOS* deacetylases may help regulate protein synthesis by deacetylating both rDNA and ribosomal protein genes.

Discussion

Acetylation microarrays have helped us to determine that *RPD3* and *HDA1* have the greatest effect on promoter deacetylation genome-wide and have shown that for the most part, the promoters most strongly deacetylated by Rpd3 differ from those strongly affected by Hda1. However, the recruitment mechanisms involved at most genes are not those (Ume6 for Rpd3 and Tup1 for Hda1) commonly believed to recruit the deacetylases. These novel recruitment mechanisms targeting Rpd3 and Hda1 to most loci remain to be discovered. Our data also argue that different histone sites of acetylation have different functions in gene regulation. In particular, acetylation of H4 lysines K5 and K12 and to

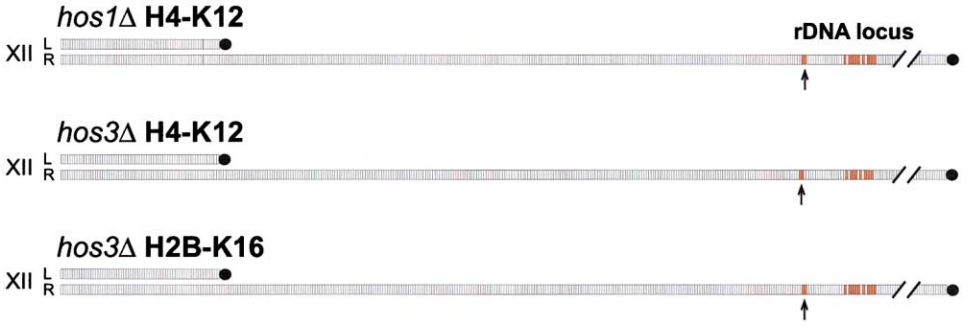

Figure 6. *HOS1* and *HOS3* Affect the Acetylation of Histones in rDNA

Chromosomal display of regions that are affected by *hos1*Δ at histone H4-K12 or *hos3*Δ at histone H4-K12 or H2B-K16. Left (L) and right (R) chromosome 12 (XII) arms are represented from their telomere end to their centromere (black circle) as described in Figure 3. Sites whose enrichment is increased (>1.95) relative to the wt control are shown as red boxes. These locate the rDNA locus and two adjacent orphan regions (arrows).

a lesser extent H3 K18 in the *rpd3*Δ strain correlates better with increased transcription than acetylation of H4 site K16. Yet H4 K16 is acetylated in euchromatin of wild-type yeast cells and is the only H4 site acetylated in monoacetylated histone H4 (Clarke et al., 1993; Suka et al., 2001). It is possible that H4 K16 genome-wide acetylation has a function that is different from those of the other H4 sites. Since unacetylated H4 K16 is part of the binding site for the repressor Sir3 at telomeric heterochromatin and since H4 acetylation prevents SIR3 binding (Carmen et al., 2002), H4 K16 acetylation may prevent genome-wide promiscuous binding of the repressor Sir3.

These studies have uncovered subtelomeric HAST domains that are likely repressed by Tup1/Ssn6-mediated Hda1 deacetylation and which may represent domains of novel chromatin structure. The HAST domains, whose genes are activated under conditions of metabolic stress, are distinct from Sir-regulated telomeric and *HM* heterochromatin that is also repressed. But HAST domains may resemble heterochromatin. First, like telomeric or *HM* heterochromatin, HAST domains are hypoacetylated (in this case by Hda1) over long continuous stretches and not just over promoters. Second, many origins of replication found in the HAST domains are late firing origins, a feature also indicative of telomeric and HM heterochromatin. These include late firing origins in HAST domains of Chr. II, VI, X, XII, and XVI (Raghuraman et al., 2001; Yamashita et al., 1997). Unlike telomeric or *HM* heterochromatin that is constitutively repressed, HAST domain genes are repressed mainly under rich growth conditions and are then selectively activated under conditions of nutrient deprivation. In this respect HAST domains may resemble facultative heterochromatin whose genes are selectively activated during certain developmental stages (Richards and Elgin, 2002).

These studies have also identified targets of all HOS deacetylases. Hos2 has its greatest effect on the acetylation of ribosomal protein genes including a number of ribosomal protein ORFs. Interestingly, Rpd3 is also found in high concentrations at ribosomal protein gene promoters but not ORFs (Kurdistani et al., 2002). Despite the involvement of two histone deacetylases with ribosomal protein genes, these genes are not repressed. It is possible that these deacetylases mediate repression at a different stage in the yeast life cycle. Alternatively, deacetylases need not function only in repression of promoters. Since the acetyltransferase Elp3 is part of the transcription elongation complex (Wittschieben et al., 1999), Hos2 may reverse acetylation after passage of the polymerase complex on ribosomal protein (or other highly active) genes. This would allow the resetting of a net deacetylated global chromatin structure (Vogelauer et al., 2000). Finally, Hos1 and Hos3 deacetylate rDNA genes primarily. Since ~50% of rDNA genes are repressed (Lucchini and Sogo, 1994), Hos1 and Hos3 may regulate these genes preferentially.

The genome-wide enzyme activity maps for the HDAC family of related histone deacetylases are an important complement to both expression arrays maps resulting from HDAC deletion and those demonstrating genome-wide HDAC binding. For example, expression arrays are important in determining the sites at which gene expression is altered by deletion of the deacetylase *RPD3*. However, this approach alone is sensitive to indirect effects on transcription, and *rpd3*Δ causes more genes to be downregulated than upregulated. This has led to speculation as to the possible role of Rpd3 as an activator of transcription (Bernstein et al., 2000). However, acetylation arrays demonstrate that there is a highly significant association between sites at which *rpd3*Δ results in increased acetylation and increased transcription but not decreased transcription. Interestingly, even *BNA1*, which codes for an NAD-biosynthesis enzyme and which was described as a gene that is likely to be activated directly (as much as 10-fold) by *rpd3*Δ (Bernstein et al., 2000), does not appear to be a direct target of Rpd3 deacetylation. On the contrary, Rpd3 binding arrays show that there is little (only 1.7-fold) enrichment of Rpd3 at *BNA1* (Kurdistani et al., 2002) and our acetylation array data show that neither the *BNA1* IGR nor ORF are hyperacetylated in the *rpd3*Δ strain. Thus, *BNA1* downregulation caused by deletion of *RPD3* is likely to occur indirectly, affected by changes in expression of other genes. Given the extension of the expression array data by acetylation arrays, it is likely that Rpd3 is a direct genome-wide repressor and not

an activator of transcription. The acetylation arrays have also extended the number of genes and gene classes affected by histone deacetylases. This is evident in the overrepresentation of meiosis-specific and carbohydrate utilization gene classes in acetylation but not in expression arrays (Bernstein et al. 2000) and the identification of novel targets for Hda1, Hos1, Hos2, and Hos3 that have not been described earlier (Bernstein et al., 2000). However, it should be stressed that even together, expression and acetylation array studies may not uncover even important gene classes that are deacetylase targets. For example, despite the preferential enrichment of Rpd3 at the very large (~100) class of RP genes (Kurdistani et al., 2002), we have found little effect of *rpd3*Δ on H4 acetylation at the RP genes. This lack of increased acetylation may be due to the redundancy there between Rpd3 and Hos2 deacetylation, a situation that is more easily clarified by the use of binding arrays. Thus, expression, acetylation, and enzyme binding arrays are all important tools that are complementary in our understanding of HDAC function. In conclusion, we believe that these studies have determined the division of labor for the related family of histone deacetylases of yeast. They have uncovered the existence of novel gene classes affected by histone deacetylases, new mechanisms of deacetylase recruitment, and unique chromosomal domains affected by specific histone deacetylases. The molecular details of these interactions should now be approachable.

Experimental Procedures

Yeast Strains

Histone deacetylase mutants WJY111(Δ*hda1*), KLY55(Δ*rpd3*), and AWY1(Δ*hos2*) (Wu et al., 2001) are isogenic to YDS2 (Laman et al., 1995), whereas NSY133(Δ*hos1*) (Wu et al., 2001) and SRY45(Δ*hos3*) are isogenic to YDS21U (Rundlett et al., 1996). *HDA1* was deleted using the *hda1::KAN* disruption plasmid pWJ119 (Wu et al., 2001). *SIR2* mutant strain JRY4587 (Δ*sir2*) and its wild-type counterpart (JRY4012) were described earlier (Fox et al., 1995).

Microarrays and Data Analysis

About 6700 intergenic regions were obtained from yeast genomic DNA by PCR. Primer pairs (Research Genetics) were designed to amplify intergenic regions from the end of an ORF up to the beginning of the following ORF as indicated earlier (Iyer et al., 2001). These were checked for size by agarose gel electrophoresis. Amplified intergenic sequences were resuspended in 3× SSC and were printed on amino-silane-coated slides (Corning) using a microarrayer built according to specifications available at http://cmgm.stanford.edu/pbrown/mguide. The ORF microarrays were purchased from Corning (CMT-YEAST). Chromatin immunoprecipitation was performed as described earlier (Rundlett et al., 1998) on yeast cells grown to A600 ~1 in YEPD medium (50 ml). We used highly specific antibodies raised against individual acetylated lysines of core histone amino-terminal tails (Suka et al., 2001). Chromatin was sheared by sonication to an average size of ~500 bp. Acetylated chromatin fragments were immunoprecipitated after addition of 2–5 μl of the indicated antiserum to 50 μl of whole-cell extract (1×10^8 cells). We used 15% of the immmunoprecipitated DNA for PCR amplification as described at http://www.microarrays.org. Fluorescent label was introduced into amplified DNA (500 ng) by klenow random-priming (modified from Bioprime labeling kit [GIBCO-BRL]) as described at http://www.microarrays.org). Fluorescent probes were mixed, purified, and concentrated through a microcon-30 filter (Amicon®). Microarrays were hybridized in 5× SSC, 50% formamide, 0.2% SDS, 0.5 mg/ml tRNA, and 0.5 mg/ml salmon sperm. After an overnight hybridization at 44°C in a humid chamber, microarrays were briefly washed in 2× SSC to remove the cover slip. Then slides were subsequently washed at RT for 5 min in 0.1× SSC/0.1% SDS and twice in 0.1× SSC. Microarrays were scanned (GMS 418 Array Scanner, Genetic Micro Systems) and fluorescence intensities were quantified using Imagene™ software (version 4.1) from BioDiscovery, Inc. Acetylation data for all deacetylase mutants except *sir2*Δ were normalized against intensities at unaffected sites at telomere 6R and 9L as well as at least six other unaffected regions verified by standard ChrIP (Rundlett et al., 1998). Since Sir2 affects telomeres, *sir2*Δ data were normalized by the ratio of total intensities across the entire array between the two fluorescent dyes. All arrays were done at least twice from different ChrIP, and data were averaged for each deacetylase. Moving averages of percentile ranks in Figures 2 and 4 were done as follow. Data were sorted according to their enrichment ratio values and assigned a percentile rank from the highest to the lowest value. Ratios from the first 100 genes (window size, 100) with the highest values are averaged. The window is then progressively moved by 1 gene at a time (step, 1) along the percentile rank ordering, and the averaged ratios are reevaluated. All the averaged ratios are then plotted according to the figure legends.

Acknowledgments

We are grateful to the members of the Grunstein laboratory and to Charles West for critical comments and discussion throughout this work and to Edward Marcotte and Saeed Tavazoie for help with statistical analysis. We are especially grateful to Patrick O. Brown who made available the primer sets for the intergenic arrays and to the laboratory of Stan Nelson for technical suggestions and for the use of their microarray scanner. I.X. is very grateful to David Eisenberg for his support and encouragement. D.R. is a recipient of fellowships from the Swiss National Science Foundation and the Roche Research Foundation. S.K.K. is a Howard Hughes Medical Institute physician postdoctoral fellow. This work was supported by Public Health Service grants (GM23674 and GM42421) of the National Institutes of Health to M.G.

Received: January 24, 2002
Revised: March 29, 2002

References

Bernstein, B.E., Tong, J.K., and Schreiber, S.L. (2000). Genomewide studies of histone deacetylase function in yeast. Proc. Natl. Acad. Sci. USA *97*, 13708–13713.

Boles, E., and Hollenberg, C.P. (1997). The molecular genetics of hexose transport in yeasts. FEMS Microbiol. Rev. *21*, 85–111.

Braunstein, M., Sobel, R.E., Allis, C.D., Turner, B.M., and Broach, J.R. (1996). Efficient transcriptional silencing in *Saccharomyces cerevisiae* requires a heterochromatin histone acetylation pattern. Mol. Cell. Biol. *16*, 4349–4356.

Carmen, A.A., Milne, L., and Grunstein, M. (2002). Acetylation of the yeast histone H4 N-terminus regulates its binding to heterochromatin protein SIR3. J. Biol. Chem. *277*, 4778–4781.

Clarke, D.J., O'Neill, L.P., and Turner, B.M. (1993). Selective use of H4 acetylation sites in the yeast *Saccharomyces cerevisiae*. Biochem. J. *294*, 557–561.

Davie, J.K., Trumbly, R.J., and Dent, S.Y.R. (2002). Histone-dependent association of Tup1-Ssn6 with repressed genes *in vivo*. Mol. Cell. Biol. *22*, 693–703.

DeRisi, J.L., Iyer, V.R., and Brown, P.O. (1997). Exploring the metabolic and genetic control of gene expression of a genomic scale. Science *278*, 680–686.

De Rubertis, F., Kadosh, D., Henchoz, S., Pauli, D., Reuter, G., Struhl, K., and Spierer, P. (1996). The histone deacetylase RPD3 counteracts silencing in *Drosophila* and yeast. Nature *384*, 589–591.

Eisen, M.B., Spellman, P.T., Brown, P.O., and Botstein, D. (1998). Cluster analysis and display of genome-wide expression patterns. Proc. Natl. Acad. Sci. USA *95*, 14863–14868.

Fox, C., Loo, S., Dillin, A., and Rine, J. (1995). The origin recognition

complex has essential functions in transcriptional silencing and chromosomal replication. Genes Dev. *9*, 911–924.

Holstege, F.C.P., Jennings, E.G., Wyrick, J.J., Lee, T.I., Hengartner, C.J., Green, M.R., Golub, T.R., Lander, E.S., and Young, R.A. (1998). Dissecting the regulatory circuitry of a eukaryotic genome. Cell *95*, 717–728.

Hughes, T.R., Marton, M.J., Jones, A.R., Roberts, C.J., Stoughton, R., Armour, C.D., Bennett, H.A., Coffey, E., Dai, H., He, Y.D., et al. (2000). Functional discovery via a compendium of expression profiles. Cell *102*, 109–126.

Imai, S.-I., Armstrong, C.M., Kaeberlein, M., and Guarente, L. (2000). Transcriptional silencing and longevity protein SIR2 is an NAD-dependent histone deacetylase. Nature *403*, 795–800.

Iyer, V.R., Horak, C.E., Scafe, C.S., Botstein, D., Snyder, M., and Brown, P.O. (2001). Genomic binding sites of the yeast cell-cycle transcription factors SBF and MBF. Nature *409*, 533–538.

Kadosh, D., and Struhl, K. (1997). Repression by Ume6 involves recruitment of a complex containing Sin3 corepressor and Rpd3 histone deacetylase to target promoters. Cell *89*, 365–371.

Kadosh, D., and Struhl, K. (1998). Targeted recruitment of the Sin3-Rpd3 histone deacetylase generates a highly localized domain of repressed chromatin *in vivo*. Mol. Cell. Biol. *18*, 5121–5127.

Kurdistani, S.K., Robyr, D., Tavazoie, S., and Grunstein, M. (2002). Genome wide binding map of the RPD3 histone deacetylase in yeast. Nat. Genet. *31*, in press.

Laman, H., Balderes, D., and Shore, D. (1995). Disturbance of normal cell cycle progression enhances the establishment of transcriptional silencing in *Saccharomyces cerevisiae*. Mol. Cell. Biol. *15*, 3608–3617.

Lucchini, R., and Sogo, J.M. (1994). Chromatin structure and transcriptional activity around the replication forks arrested at the 3′ end of the yeast rRNA genes. Mol. Cell. Biol. *14*, 318–326.

Moazed, D. (2001). Enzymatic activities of Sir2 and chromatin silencing. Curr. Opin. Cell Biol. *13*, 232–238.

Raghuraman, M.K., Winzeler, E.A., Collingwood, D., Hunt, S., Wodicka, L., Conway, A., Lockhart, D.J., Davis, R.W., Brewer, B.J., and Fangman, W.L. (2001). Replication dynamics of the yeast genome. Science *294*, 115–121.

Ren, B., Robert, F., Wyrick, J.J., Aparicio, O., Jennings, E.G., Simon, I., Zeitlinger, J., Schreiber, J., Hannett, N., Kanin, E., et al. (2000). Genome-wide location and function of DNA binding proteins. Science *290*, 2306–2309.

Richards, E.J., and Elgin, S.C.R. (2002). Epigenetic codes for heterochromatin formation and silencing: rounding up the usual suspects. Cell *108*, 489–500.

Robzyk, K., Recht, J., and Osley, M.A. (2000). Rad6-dependent ubiquitination of histone H2B in yeast. Science *287*, 501–504.

Rundlett, S.E., Carmen, A.A., Kobayashi, R., Bavykin, S., Turner, B.M., and Grunstein, M. (1996). HDA1 and RPD3 are members of distinct histone deacetylase complexes that regulate silencing and transcription. Proc. Natl. Acad. Sci. USA *93*, 14503–14508.

Rundlett, S.E., Carmen, A.A., Suka, N., Turner, B.M., and Grunstein, M. (1998). Transcriptional repression by UME6 involves deacetylation of lysine 5 of histone H4 by RPD3. Nature *392*, 831–835.

Strahl-Bolsinger, S., Hecht, A., Luo, K., and Grunstein, M. (1997). SIR2 and SIR4 interactions differ in core and extended telomeric heterochromatin in yeast. Genes Dev. *11*, 83–93.

Suka, N., Suka, Y., Carmen, A.A., Wu, J., and Grunstein, M. (2001). New antibodies for sites of acetylation determine novel histone site usage in heterochromatin and euchromatin. Mol. Cell *8*, 473–479.

van Helden, J., Andre, B., and Collado-Vides, J. (2000). A web site for the computational analysis of yeast regulatory sequences. Yeast *16*, 177–187.

Vannier, D., Balderes, D., and Shore, D. (1996). Evidence that the transcriptional regulators SIN3 and RPD3, and a novel gene (SDS3) with similar functions, are involved in transcriptional silencing in *Saccharomyces cerevisiae*. Genetics *144*, 1343–1353.

Vogelauer, M., Wu, J., Suka, N., and Grunstein, M. (2000). Global histone acetylation and deacetylation in yeast. Nature *408*, 495–498.

Watson, A.D., Edmondson, D.G., Bone, J.R., Mukai, Y., Yu, Y., Du, W., Stillman, D.J., and Roth, S.Y. (2000). Ssn6-Tup1 interacts with class I histone deacetylases required for repression. Genes Dev. *14*, 2737–2744.

White, D.A., Belyaev, N.D., and Turner, B.M. (1999). Preparation of site-specific antibodies to acetylated histones. Methods *19*, 417–424.

Wittschieben, B.O., Otero, G., de Bizemont, T., Fellows, J., Erdjument-Bromage, H., Ohba, R., Li, Y., Allis, C.D., Tempst, P., and Svejstrup, J.Q. (1999). A novel histone acetyltransferase is an integral subunit of elongating RNA polymerase II holoenzyme. Mol. Cell *4*, 123–128.

Wu, J., Suka, N., Carlson, M., and Grunstein, M. (2001). TUP1 utilizes histone H3/H2B-specific HDA1 deacetylase to repress gene activity in yeast. Mol. Cell *7*, 117–126.

Yamashita, M., Hori, Y., Shinomiya, T., Obuse, C., Tsurimoto, T., Yoshikawa, H., and Shirahige, K. (1997). The efficiency and timing of initiation of replication of multiple replicons of *Saccharomyces cerevisiae* chromosome VI. Genes Cells *2*, 655–665.